

# Sensing using Eigenchannels in Radio-Frequency Multiple-Input, Multiple Output Communication Systems

Nicolas Bikhazi, William F. Young, Hung Nguyen  
 Sandia National Laboratories, Albuquerque, NM, USA

## ABSTRACT

This paper describes the use of multiple-input, multiple-output (MIMO) communication technology as a radio frequency (RF) sensor. We suggest some possible measures for determining how the changes in MIMO channel are related to objects moving through the MIMO channel. Initially, we examine the singular values of the channel matrix. We further demonstrate the effects of the signal-to-noise ratio (SNR) in conjunction with the target physical properties in the creation of eigenchannels. These eigenchannels represent the key factor in the ability of a MIMO system to perform as an effective sensor. Another important feature of MIMO technology is that it allows us to capture spatial information about the target, beyond the typical time and frequency information. Preliminary experimental results at 750 MHz demonstrate that targets can be detected and distinguished based on these simple measures. For example, a vehicular target is distinguishable from a person or groups of people.

Our concept is closely related to a MIMO radar approach. However, a key difference is that we make use of the natural process of establishing a MIMO communication link rather than interrogate a specific physical region via a pulsed RF waveform. MIMO communications requires sounding of the physical environment and the creation of a channel matrix in order to maximize data throughput. We leverage this information about the area of interest already captured by the communication system. This allows the use of a MIMO system for both sensing and communication.

**Keywords:** MIMO sensor, MIMO radar, personnel detection

## 1. INTRODUCTION

The general concept of using multiple-input, multiple-output (MIMO) technology for radar systems is an area that is currently seeing a great deal of attention in the research community.<sup>[1][2]</sup> Other communication concepts such as orthogonal frequency-division multiplexing<sup>[3]</sup> ultra-wide band<sup>[4]</sup> are also under investigation for application to radar systems. The benefits to communication systems by the technologies mentioned above and MIMO in particular, are well known as evident in the use of MIMO techniques in the IEEE 802.11n<sup>[5]</sup>, and 3rd Generation Partnership Project Long Term Evolution<sup>[6]</sup> standards. Investigations of the benefits from MIMO to specific systems include detecting personnel in urban<sup>[7]</sup> and wooded<sup>[8]</sup> environments, and enhancing the ability of radar in penetrating building walls<sup>[9]</sup>.

We take a slightly different perspective than the radar centric view above, and treat the environment around the object of interest as a communication channel between two wireless devices. The object of interest then perturbs the channel while moving through the channel. We focus on two measures of the channel matrix, the singular values and the channel capacity. This perspective supports using the inherent signaling that is required to setup a MIMO communication channel. Thus, the MIMO communication device serves as both a sensor and a communication device.

The remainder of the paper proceeds as follows: Section 2 offers a basic theoretical description of the MIMO sensing process; Section 3 includes results from some initial experiments testing the MIMO sensor concept; and finally, in Section 4 we draw some conclusions based on these experiments.

## 2. BASIC THEORETICAL DESCRIPTION OF THE EIGENCHANNEL

### 2.1 Mathematical Concept

The fundamental aspect of this work is in the analysis of the MIMO channel matrix. The basic approach to MIMO signaling exploits the multiple channels available within the channel matrix. However, in order to optimize the data

throughput, a MIMO system must preprocess the transmitted signal, and post process the received signal. This requires knowledge of the channel, as well as various mathematical manipulations on that channel information, which is described in detail by Durgin.<sup>[10]</sup>

An  $M \times N$  MIMO communication system has  $M$  transmitting elements and  $N$  receiving elements. The equation (without including the noise contribution) that describes this time dependency of this system is written as:

$$\vec{y}(t)_{N \times 1} = \frac{1}{2} \bar{H}(t)_{N \times M} \vec{x}(t)_{M \times 1} \quad (1)$$

where  $\vec{y}$  is the received signal vector,  $\vec{x}$  is the transmitted signal vector, and  $\bar{H}$  is the channel matrix. For simplicity, we only focus on the time varying aspect of the channel, which represents the key channel parameter in our approach. The MIMO device generates the channel matrix  $\bar{H}$  by sounding the channel, (as will be described in the experimental setup). Once  $\bar{H}$  is known, a singular value decomposition (SVD) is performed to determine the eigenvalues associated with each of the individual channels. We can write  $\bar{H}$  as,

$$\bar{H}_{N \times M} = \bar{U}_{N \times N} \bar{D}_{N \times M} \bar{V}_{M \times M}^* \quad (2)$$

where  $\bar{U}$  and  $\bar{V}$  are unitary matrices, (i.e.,  $\bar{V}\bar{V}^* = \bar{I}$ ), and  $*$  means the conjugate transpose. From SVD theory, the nonzero diagonal elements of  $\bar{D}$ , when squared, are the eigenvalues of the matrix  $\bar{H}^* \bar{H}$  when  $N \geq M$  or of the matrix  $\bar{H} \bar{H}^*$  when  $M \geq N$ .

These eigenvalues are associated with what can be viewed as a channel between the transmitter and receiver, and indicate how to distribute the power amongst the channels in order to maximize the data throughput using a water-filling technique. Equations (2) and (3) in the paper by Goldsmith, et al, <sup>[11]</sup> are repeated here to support analysis and discussions in the paper. The equation for capacity,  $C$  is

$$C = \max_{Q: Tr(Q) = P} \log |\bar{I}_N + \bar{H} \bar{Q} \bar{H}^*| \quad (3)$$

where  $\bar{Q}$  is the input covariance matrix, and  $Tr(\bar{Q})$  is the trace of  $\bar{Q}$ . The power allocation for the waterfilling strategy is then described as

$$P_i = \left( \mu - \frac{1}{\sigma_i^2} \right)^+, 1 \leq i \leq \min(M, N) \quad (4)$$

where  $\mu$  is the waterfill level,  $\sigma_i^2$  is the  $i$ th singular value,  $P_i$  is the power in the  $i$ th eigenmode of the channel, and  $(x)^+$  is defined as  $\max(x, 0)$ .

In our case, we are not interested in the capacity of the MIMO system for data transfer, but rather to observe how  $\bar{H}$  changes over time. Thus, we consider two key properties of  $\bar{H}^* \bar{H}$  (or  $\bar{H} \bar{H}^*$ ), the singular values, and the channel capacity. We also examined the condition number of  $\bar{H}^* \bar{H}$  since this could perhaps provide a very simple method of detection. However, due to the line-of-site nature of these current experiments and the dynamic range of our measurement system the smallest singular values likely corresponds to noise, and thus does not provide obvious meaningful results.

## 2.2 Experimental Setup

The goal for this experiment was to illustrate the advantages a MIMO system to detect and identify nearby targets. Additionally, we wished to mimic a communication environment somewhat similar to commercial off the shelf hardware. Thus, we used a channel sounding technique described in the paper by Wallace and Jensen<sup>[12]</sup>.

The transmitter and receiver were placed 25 yards apart with a fairly open line of sight channel. The transmitter consisted of four unique binary phase shift keying baseband signals generated with a field programmable gate array. Each signal was transmitted continuously at a 4MBPS rate. To simplify channel sounding, each channel synchronously transmitted 8 symbols of identical training data followed by an 8 symbol orthogonal Walsh code. The receiver locked onto the training data, and then determined the actual 4x4 channel by correlating against the orthogonal Walsh codes. These baseband signals were then each mixed with a 746 MHz RF source and fed to an antenna array. The antenna array was made with 4 monopole elements separated by a half wavelength (0.2 m).

The receiving system directly sampled elements of an identical array via synchronized 4 channel 1GS/s Gage cards [13]. 1GS/s sampling and a center transmit frequency of 750 MHz yielded a subsampled configuration, which is no impediment to this work. The direct sampling simplified the receiving system. The data was then read from the Gage cards and stored on a hard drive for post processing computation of the actual channels. Since the memory on the sample cards was limited, the transmitted data was captured only 15ms at a time. Each capture of the data occurred at 1/3 s intervals for a total duration of 40 s per measurement (see Figure 1).

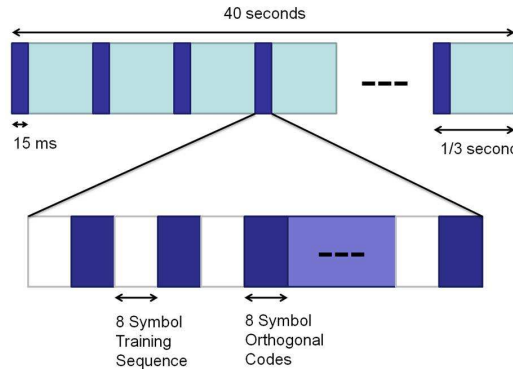


Figure 1. Illustration of the time intervals for capturing the channel. Data was captured for 15 ms every 333 ms.

## 2.3 Measurement Scenarios

A total of ten measurements were taken with both walking people targets and a moving van. Table 1 describes the target scenarios, and Figure 2 shows the paths taken by various targets traveling throughout the channel with respect to the transmitter and receiver. The target's location was tracked with 1Hz GPS location updates. The paths based on GPS tracking are also shown in Figure 2, along with the transmitter and receiver.

## 2.4 Singular Value Results

Plots of these singular values for each measurement scenario are shown in Figures 3 and 4. Recall that multiple channels were captured every 1/3 of a second, and thus the blocky nature is due to gaps in the channel sampling. However, correlation between similar target scenarios is evident.

Table 1. List of measurement scenarios.

Measurement Number	Description
1	Van moving from east to west at 5 mph in between transmitter and receiver.
2	A repeat of Test 1.
3	Van moving from east to west at 5 mph behind receiving platform.
4	A repeat of Test 3.
5	Person walking east to west at a near constant speed.
6	A repeat of test 5.
7	Person walking east to west behind receiving platform.
8	Person walking diagonal between the transmitter and receiver.
9	A group of three people walking from east to west between transmitter and receiver.
10	A repeat of test 6.

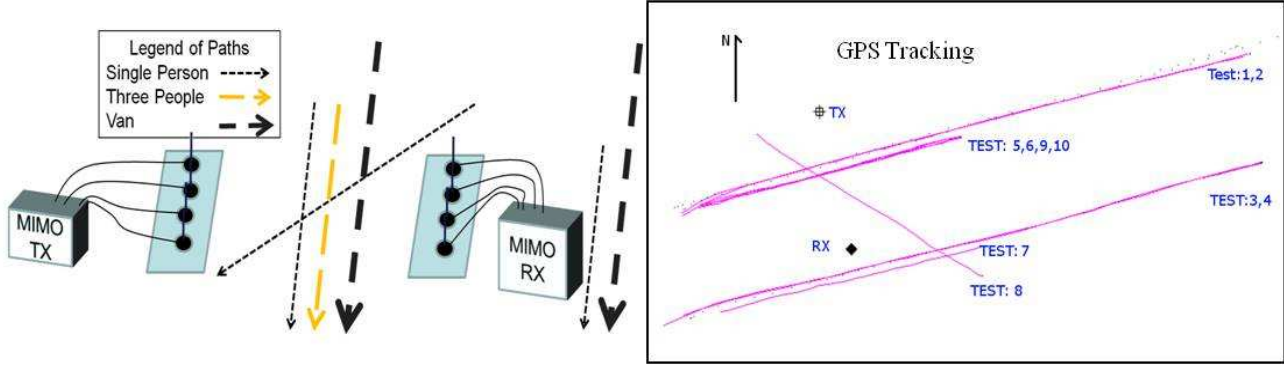


Figure 2. Illustration of the MIMO channel and various paths. The GPS tracking shows the actual paths covered in for a given measurement, as well at the locations of the MIMO transmitter (TX) and receiver (RX).

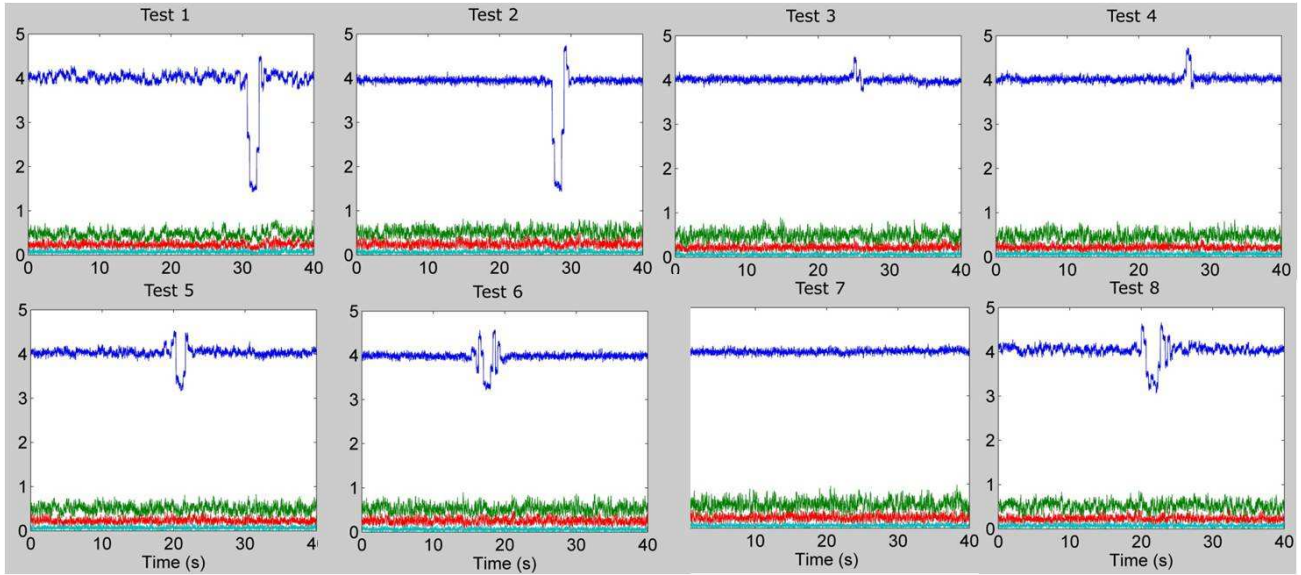


Figure 3. Singular values with a van in the channel (tests 1-4), and a person in the channel (5-6).

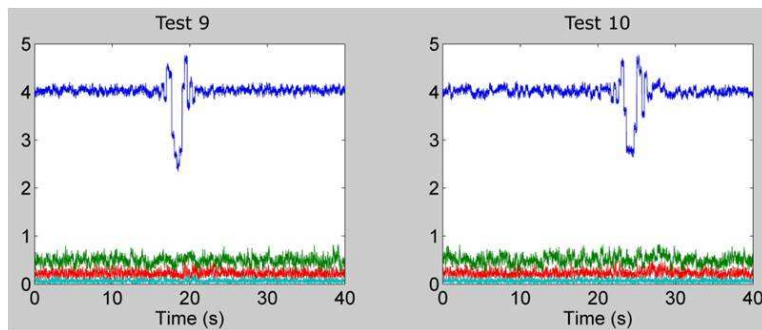


Figure 4. Singular values with a group of three people in the channel.

Visual comparison of the dominant singular value illustrates a high level of correlation for the van as a test target. Signatures obtained from tests 1 and 2 appear to correlate well with each other, likewise between tests 3 and 4. Also, the dominant singular value fell with tests 1 and 2 and peeked with tests 3 and 4. As expected, these signatures yield an obvious difference between the measurements.

Power in the channel (or rather the lack of attenuation in the channel) can be seen in a norm of the channel matrix. Since this channel is nearly a LOS channel a norm of the channel matrix is dominated by the first singular value. Hence, the attenuation seen of the dominant singular value in tests 1 and 2 is due to the van being in between the transmitters blocking the signal. Also, in tests 3 and 4 a gain in the norm is seen due to a large reflector passing behind the receiver and thus increasing the power to the device.

Consider in tests 1 and 2 the sudden spike in channel power after the deep attenuation of the van blocking the signal. These gain spikes occur at 32 and 29 seconds in test 1 and 2 respectively and are not apparent at the beginning of the attenuation. This gain may be due to a strong reflection from the back of the van, which is fairly flat and mostly metal. The front of the van has smoother edges, a plastic grill, and the engine compartment sticks out in front of the front windshield by about 2 feet yielding a less uniform surface.

The targets with a single person involved (tests 5-8), though unique when compared against the van measurements, are not visually as well correlated one to another, though there are some similarities. The strongest similarity between all of the person tests where the person walked between the transmitter and receiver is the level of attenuation. However, the oscillations of the dominant singular values appear to not match perfectly well between the tests. This could indicate a need for a quicker sampling of the channel than once every 1/3 second. It is not surprising that test 7 has hardly any signature during the measurement as there isn't any reason a human body would reflect much energy at 750MHz.

Tests 9 and 10 appear to look similar compared to each other. There are multiple oscillations that may be similar between the two tests and the peak amplitude attenuation of the dominant singular values appears similar. In comparison, with the other tests they are fairly distinct, especially in amplitude.

## 2.5 Eigenchannel and Capacity Results

In addition to the visually obvious signatures that are present by the dominant singular value of the multipath, there are hints that multiple channels are formed in this environment. For example consider the second and third singular values of test 1 from 32 to 35 s. Something is going on, but visual inspection is really insufficient to draw any type of conclusions. One reason for this is likely the behavior of multipath channels. For each channel matrix realization, the eigenvectors (i.e., multichannel beam weights used to pre and post-condition the transmitted data) are unique for that channel. These eigenvectors determine where the energy is placed spatially and thus likely spatial information useful for target identification. Detailed analysis of the inherent spatial information is beyond the scope of this paper; however, we apply a related concept, namely channel capacity.

The channel capacity used in this paper, via equation (3), assumes that some level of channel state is known both at the transmitter and at the receiver. This capacity is not always achievable in a practical sense. However, this measure has the advantage for mixing different amounts of multipath together through setting the average transmitted power level and maximizing equation (3) in Section 2 through waterfilling described by (4). Therefore, by setting  $\mu$  to a low level only one eigenchannel will be used. Also, by raising the average power level, an increasing number of eigenchannels will be used in the capacity expression.

To observe capacitive signatures from our measurements equation (3) and (4) were used with various average power levels. Cross-correlation was performed between each test taken. (Note: as the peak signatures didn't occur at the exact same time in each of the tests time shifts were used to maximize the magnitude of the cross-correlation coefficient.) These cross-correlation coefficients for various waterlevels are shown in Figure 5. Additionally, the average number of eigenchannels used for all tests (N) and the signal to noise ratio (SNR) used is also shown. This SNR is a relative term for this work to illustrate how much power is needed to change the various waterfilling levels.

Figure 5 shows that with  $N=1.0$  there is significant coupling between tests 1 and 2, between tests 5, and 6 and between tests 9 and 10. With  $N = 1.0$ , capacity is very similar to dominant singular value plots shown in Figures 3 and 4. Therefore, it is not a surprise that there is such well coupling between these events. However, there appears to be a large amount of coupling between tests that look significantly different. For example, the group 1 and 2 seem to couple well with tests group 9 and 10.

As the waterfilling level is raised this interdependency between groups diminishes. When the  $N$  is raised to 2.7 the correlation between any test virtually disappears. This is likely due to the weaker eigenchannels being more of a measurement of noise rather than actual multipath present. (This is based upon the safe assumption that the measurement system noise is fairly white). Considering that the dynamic range for the Gage cards was only 8-bits (which were not governed by an automatic gain control) it is likely there may have been multipath present, but that it

was simply below the capability of this system to measure. In this light the correlation that is present, when  $N = 2.7$ , between test 1 and 2 is peculiar. This hints that there may be a spatial multipath signature between tests 1 and 2 that isn't plainly visible in Figure 4.

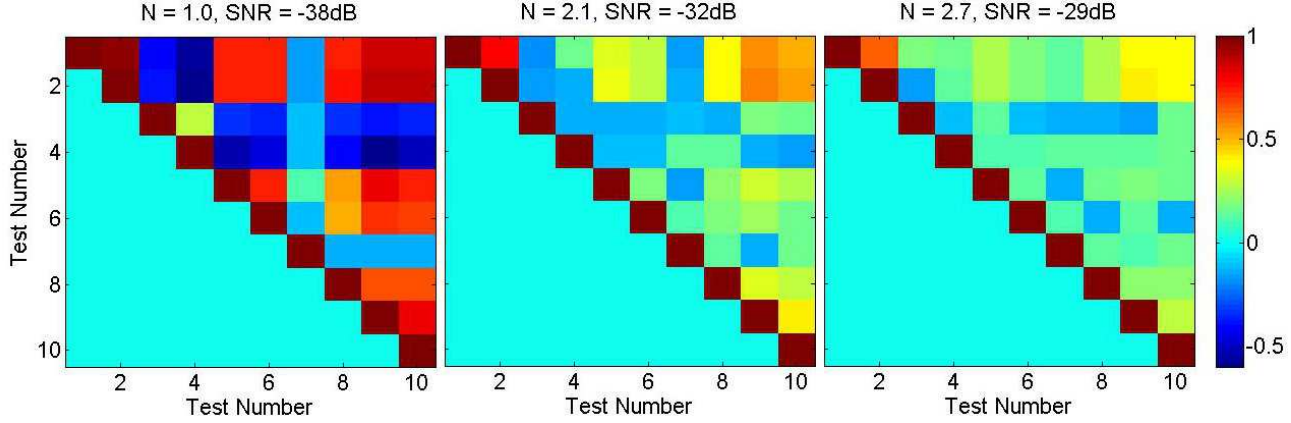


Figure 5. Cross-correlation coefficients for three average power levels. Value indicated by the color bar.

### 3. CONCLUSIONS

The basic conclusion of this work is that singular value inspection and capacity calculations may support object detection in a MIMO channel. It appears that using multiple eigenchannels in a signature may also be a valid method for target characterization. The results support further investigation of MIMO communication technology as a viable sensor.

### REFERENCES

- [1] Bliss, D.W. and Forsythe, K.W., "Multiple-input multiple-output (MIMO) radar and imaging: degrees of freedom and resolution," Conference Record of the Thirty-Seventh Asilomar Conference on Signals, Systems and Computers, 54- 59 (2003).
- [2] Chernyak, V.S., "MIMO radars. What are they?," 2010 European Radar Conference (EuRAD), 137-140, (2010).
- [3] Donnet, B.J. and Longstaff, I.D., "Combining MIMO Radar with OFDM Communications," EuRAD 2006: 3rd European Radar Conference, 37-40, (2006).
- [4] Shingu, G., Takizawa, K. and Ikegami, T., "Human Body Detection Using MIMO-UWB Radar Sensor Network in an Indoor Environment," PDCAT 2008. Ninth International Conference on Parallel and Distributed Computing, Applications and Technologies, 437-442, (2008).
- [5] <http://standards.ieee.org/getieee802/download/802.11n-2009.pdf>
- [6] <http://sites.google.com/site/teencyclopedia/home>
- [7] Deiana, D., Kossen, A. S. and van Rossum, W. L., "Multipath exploitation in an urban environment using a MIMO surveillance radar," 2010 11th International Radar Symposium (IRS), 1-4, (2010).
- [8] Lane, R.O. and Hayward, S.D., "Detecting personnel in wooded areas using MIMO radar," IET International Conference on Radar Systems, 2007, 1-5, (2007).
- [9] Boudamouz, B., Millot, P. and Pichot, C., "Through the wall MIMO radar detection with stepped frequency waveforms," 2010 European Radar Conference (EuRAD), 400-402, (2010).
- [10] Durgin, G. D., [Space-Time Wireless Channels], Prentice Hall PTR, Upper Saddle River, NJ, (2003).
- [11] Goldsmith, A., Jafar, S.A., Jindal N., and Vishwanath, S. , "Capacity limits of MIMO channels," IEEE Journal on Selected Areas in Communications, 21(5), 684-702, (2003).
- [12] Wallace, J. W. and Jensen, M. A., "Spatial characteristics of the MIMO wireless channel: Experimental data acquisition and analysis," in Proc. IEEE Intl. Conf. Acoustics, Speech, Signal Processing (ICASSP), 4,774-779, (2001).
- [13] Cobra CompuScop 21G8 GaGe Cobra™,  
<http://www.wuntronic.eu/index.php?site=2&xid=65&subid=185&sub2id=186&pid=255>